AIAA JOURNAL
Vol. 34, No. 7, July 1996

Analytical and Experimental Comparison of Probabilistic and Deterministic Optimization

G. Maglaras,* E. Ponslet,† R. T. Haftka,‡ E. Nikolaidis,§ P. Sensharma,† and H. H. Cudney¶
Virginia Polytechnic Institute and State University, Blacksburg, Virginia 24061

The objective of this paper is to evaluate experimentally the gain in reliability that can be achieved in the design of a system by using probabilistic optimization instead of deterministic optimization. The design of a truss structure, equipped with tuned dampers and subject to constraints on the dynamic response amplitudes, is used for the investigation. The locations of the dampers and of tuning masses added to the truss are used as design variables. The properties of the dampers are the main sources of uncertainties. The deterministic and probabilistic optimizations are performed with genetic algorithms. Probabilities of failure are measured in the laboratory by testing multiple realizations of deterministic and probabilistic optimum designs. Predicted and measured values of the reliabilities of the concurrent designs are compared. For a design problem selected to maximize the contrast in reliability between the two optimum designs, the probabilistic optimization provided a large improvement in reliability compared with the deterministic optimum design. This improvement was confirmed by experiments.

Introduction

STRUCTURAL design optimization is usually based on analytical models, which depend on geometric, loading, and material properties. These properties are random in nature, and accordingly the performance of the structure is uncertain. In deterministic optimization the uncertainty in performance is compensated for by safety factors, but this approach can lead to either unreliable or overdesigned systems. Probabilistic optimization, on the other hand, attempts to use knowledge about the statistics of the uncertainties in the system to predict—and minimize—the probability of violating given performance requirements.[1]

Several studies have shown analytically that probabilistic optimization provides safer designs than deterministic optimization.[2–4] However, because of incomplete knowledge of probability distributions and of modeling uncertainties, we can only predict a nominal probability of failure, which can be significantly different from the actual one.[5,6] Experiments are then needed to answer the important question, whether probabilistic optimization based on such nominal probabilities of failure can still yield better designs than deterministic optimization.

To our knowledge no such experimental comparison between deterministic and probabilistic optimization has been performed yet. This may be because to verify safety experimentally we need to measure the performance of a large number of random realizations of deterministic and probabilistic designs corresponding to the same design problem. This could be difficult, since we would have to build, compare, and possibly destroy a large number of sample structures.

In this paper we employ an experimental setup that allows us to compare probabilistic and deterministic optimization with inexpensive, nondestructive experiments. To reduce the number of experiments needed to measure the difference in probability of failure between the two designs, we identify design problems that maximize the contrast between the two approaches. To achieve this, we use a process known as antioptimization[7–11] or contrast maximization.

Our demonstration problem is a truss with passive dampers, where the main source of response uncertainty is the variability in the properties of the nominally identical dampers. The uncertainties are quantified by measuring the properties of a large number of dampers. We compare experimentally the probabilities of failure of two alternative designs, one obtained from deterministic optimization and the other from probabilistic optimization. The design requirements are expressed as upper limits on the acceleration at given points on the structure and within prescribed frequency ranges, for a given excitation. Both designs are subject to the same requirements and resource limits. Probabilities of failure are measured by testing multiple realizations of the structure assembled with different dampers. This procedure allows us to circumvent the problem associated with the excessive cost and labor that is required when comparing probabilistic and deterministic optimization, because it is relatively easy to construct many nominally identical dampers and test them on the truss structure. The probabilistic and deterministic optimizations as well as the antioptimization are performed using genetic algorithms.

In the rest of the paper, we first describe briefly the truss and dampers used in this study, their respective models, and the analysis techniques for estimating the vibration amplitude and probability of failure of a truss design. The alternative formulations of the deterministic and probabilistic optimization problems are presented next. Then the experimental procedure for comparing the deterministic and probabilistic designs is described. Finally an approach that reduces the sensitivity of the probabilistic optimum design to modeling errors is presented.

System Description

The structure used in this study is shown in Fig. 1. It is a short, beamlike truss assembled from 30 tubular aluminum members with steel end fittings, connected through 12 spherical aluminum nodes. The truss is about 1 m (40 in.) long and weighs about 4.4 kg (9.6 lb). Three nodes are attached to a base made of thick steel and aluminum plates mounted on the laboratory wall. Detailed description of the truss can be found in Ref. 12.

The first three natural frequencies of the truss are about 100, 130, and 193 Hz. Local bending modes occur at frequencies equal to or higher than 280 Hz. Our truss model neglects bending, and therefore it is useful only for the first three modes. The inherent damping in the second mode is much higher than in the other two modes. This is attributed to coupling between the structure and the wall, which is not included in our analytical model. For that reason, only modes 1 and 3 are considered in this study.

Received Feb. 18, 1995; revision received July 12, 1995; accepted for publication July 12, 1995.

*Graduate Research Assistant, Department of Aerospace and Ocean Engineering.

†Postdoctoral Researcher, Department of Aerospace and Ocean Engineering. Member AIAA.

‡Christopher Kraft Professor, Department of Aerospace and Ocean Engineering; currently Professor, Department of Aerospace Engineering, Mechanics and Engineering Science, University of Florida, Gainesville, FL 32611. Associate Fellow AIAA.

§Associate Professor, Department of Aerospace and Ocean Engineering. Member AIAA.

¶Associate Professor, Department of Mechanical Engineering. Member AIAA.

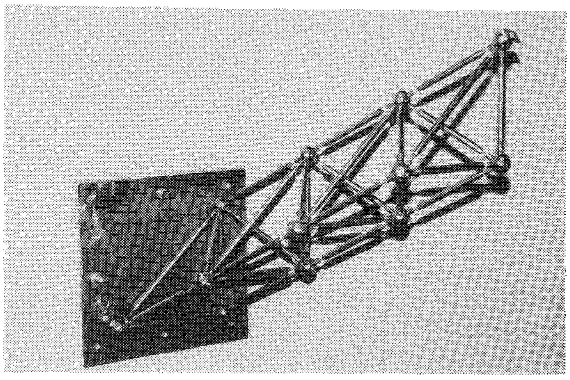

Fig. 1 Laboratory truss.

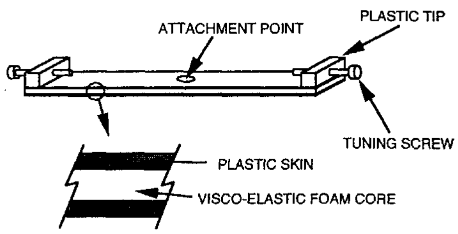

Fig. 2 Tuned damper design.

The structure is equipped with tuned dampers to reduce the dynamic response of the first and third modes. The tuned dampers were specially designed for this study. They consist of symmetric cantilevered beams that carry adjustable tip masses and are attached at their middle point to a node of the structure. The first bending mode of the beams is tuned to a natural frequency of the truss to maximize the energy that the tuned dampers absorb.

Figure 2 is a schematic sketch of a tuned damper. The beam is a sandwich of two thin plastic sheets and an inner core of viscoelastic acrylic foam. A plastic tip block is glued to one of the plastic layers at each end of the beam. A steel tuning screw is threaded into each of these blocks. This allows the fundamental frequency of the damper to be adjusted by moving the center of gravity of the tip masses in and out.

Two slightly different versions of this design (we will refer to them as type-1 and type-3) are used to target the first and the third natural frequencies of the structure. Type-1 can be adjusted from about 98 Hz to about 116 Hz; the range for type-3 is about 170–204 Hz.

The mass of the dampers is very small compared with the mass of the structure. Both types weigh about 10 g, which represents about 0.2% of the total mass of the truss. Despite their size, these dampers provide very significant damping to the truss. For example, adding one type-3 damper to the structure in a quasioptimal manner (i.e., tuned to the frequency of mode 3 and located at the node and the direction that correspond to the largest amplitude of vibration in the third mode shape) makes the amplitude in mode 3 more than 20 times smaller.

Note that the natural frequency of the damper is the most important parameter to determine its effectiveness. The tuned damper does not significantly affect modes of the truss that are far from the tuned frequency of the damper. This implies that at least one damper per target mode is needed.

Modeling and Analysis Techniques

Truss Structure Model

Each member of the structure is modeled as a six-degree-of-freedom (DOF), three-dimensional rod finite element defined by its mass and complex stiffness $k(1 + i\eta)$, where k is the stiffness and η is the loss factor of the member used to model inherent damping. The bending stiffness of the rod elements is zero. Consistent mass matrices are used to represent inertial properties of the members. Each node is modeled as an infinitely stiff concentrated mass equal to the measured mass of the physical node.

The values used in the model for the masses of the members and nodes and for the stiffnesses of the members are the mean values of

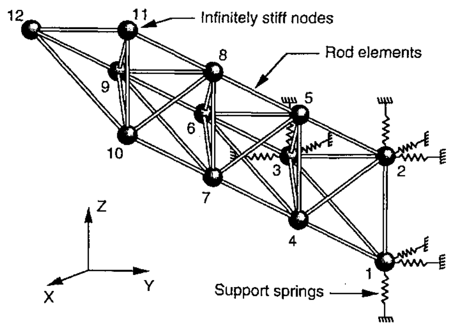

Fig. 3 Finite element model of the truss.

series of measurements performed on a large number of members and nodes. Details on these measurements can be found in Ref. 12. The flexibility of the base (wall) is simulated in the finite element model of the structure with nine springs with complex stiffnesses (three per attached node, one normal to the base, and two in the plane of the base), as shown in Fig. 3. With these support springs, the finite element model of the truss contains 36 DOF.

Tuned Damper Model

A simplified two-DOF model was devised for the tuned dampers. This model consists of two masses—a base mass m_0 attached to the node and a tip mass m—which are connected with a spring of complex stiffness $k(1 + i\eta)$. Four parameters are needed to completely define the damper model. The total mass m_T, the tip mass m, the natural frequency f_n, and the loss factor η representing the damping effect of the viscoelastic layer will be used in this study.

Except for the total mass that can be measured on a scale, these parameters are not directly measurable because of the simplifications used in the model. To estimate the remaining three parameters the damper is attached to the moving coil of an electromagnetic shaker (MB Electronics, model EA1500) and the transfer function from base acceleration to base force is measured using a sine dwell technique. A three-parameter least-squares fit is then performed using MATLAB[13] on the imaginary part of the measured transfer function and provides estimates for m, f_n, and η. Details on the experimental setup used for measuring the parameters of the tuned dampers are given in Ref. 12.

To include the tuned damper in the finite element model of the truss, we created a special four-DOF element. This element models the dynamics of the damper in the direction orthogonal to the sandwich beam, as well as the added mass effect in the other directions. Each damper adds one DOF to the model of the structure. The remaining three DOFs correspond to the three components of displacement of the node to which the damper is attached and are shared with the existing model of the truss. With two dampers on the truss, the number of degrees of freedom increases to 38.

Evaluation of Peak Response

The design requirements are related to the largest accelerations at specific nodes under unit excitation and within prescribed frequency windows. These peak accelerations are evaluated in the frequency domain using the following numerical procedure: the frequency response function (FRF) from excitation force to response acceleration is computed using the mode superposition method, which is described next. The magnitude of the FRF is evaluated numerically with a relatively coarse step size within the frequency window of interest. The peak is first located approximately using a simple slope-reversal search (the slope is approximated with forward differences). The location of the peak and the corresponding value of the FRF are then refined by second-order interpolation between the approximate peak and the two neighboring points in the FRF.

Two-Mode Approximation

The mode superposition method mentioned earlier requires the first few eigenvalues and eigenvectors of the truss with tuning masses and dampers. Obtaining exact eigenvectors and eigenvalues for a truss with two dampers requires solving a generalized

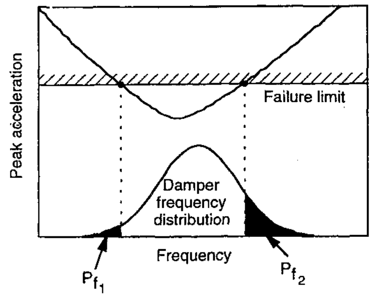

Fig. 4 Existence of multiple failure regions for a truss equipped with tuned dampers with random parameters.

complex eigenproblem with 38 DOF. The computational expense associated with this operation is prohibitive in the context of genetic optimization.

To reduce computational expenses, we use an approximate two-mode model that is valid when no more than one damper is used for each structural mode. It uses a reduced basis made of one mode (either first or third, depending on the frequency of the peak) of the truss without damper plus one Ritz vector. The Ritz vector contains zeros everywhere except at the DOF associated with the damper. An analytical expression for the frequency response function from excitation force to response acceleration is easily derived for the resulting two-DOF model and is used instead of the numerical eigensolution and mode superposition method. This analysis has to be repeated with a different basis for each mode of interest but avoids the numerical solution of the eigenvalue problem. It is about 50 times faster than the full analysis. The associated error is about 10%.

Probabilistic Analysis

For the probabilistic optimization, we need to evaluate repeatedly the probability of failure of the system. Failure occurs when the acceleration at given points on the structure exceeds a prescribed limit value (see the section titled Deterministic and Probabilistic Design Formulations for details). The amplitude (or acceleration) of vibration near resonance of a structure is highly nonlinear in the structural parameters. For that reason, a mean-value-based first-order covariance propagation method cannot be used.[14] In addition, because of the complex, nonlinear relationship between the parameters of a tuned damper and the magnitude of the peak response of a truss equipped with that tuned damper, failure can occur at both tails of the damper distribution [multiple most probable failure points (MPFP)]. This is illustrated in Fig. 4, which shows a hypothetical distribution of the natural frequency of a tuned damper. The other curve in the figure shows the peak amplitude of the structural mode as a function of the damper natural frequency. The total failure probability is the sum of the probability of failure of the two MPFPs. However, a second moment method may grossly underestimate the probability of failure, because it finds only one MPFP. There is no guarantee that a second moment method will find the MPFP that has the largest probability of failure. Furthermore, there are situations where failure probabilities of both MPFP must be taken into account. Therefore, although second moment methods are faster, we used Monte Carlo simulation to evaluate the probabilities of failure.

In general, Monte Carlo simulation is expensive computationally and can be used only when the cost for one analysis is small. In our study the problem is relatively simple and use of the two-mode approximation makes Monte Carlo simulation affordable. For more complicated problems, other methods such as integrated analysis and design (e.g., Ref. 15) and methods using response surface polynomials to estimate the response of the structure for many values of the random variables and the design variables (e.g., Ref. 16) can be used.

To evaluate the required sample size N, we used the formula[17]

$$N = \frac{1-p}{pCOV_p^2} \tag{1}$$

where p is the anticipated probability of failure and COV_p the desired coefficient of variation (defined as the standard deviation divided by the mean) of the probability of failure. In this study, we work with probabilities of failure of the order of 0.1, and we accept a coefficient of variation of 0.1. Substituting these values in the preceding formula, we get that the minimum value of N must be 900. We chose a sample size of 1000. The standard deviation in the evaluated probabilities of failure associated with that sample size is then[17]

$$\sigma_p = \sqrt{\frac{p(1-p)}{1000}} \tag{2}$$

Because the total mass of the dampers has very little scatter, it was assumed deterministic in the simulations. The three remaining parameters (natural frequency f_n, tip mass m, and loss factor η) of each damper were found to be approximately normally distributed random variables. Their mean values, standard deviations, and coefficients of correlation were evaluated from series of tests (see the Results section). A complete 1000-point Monte Carlo simulation uses about 12 s of CPU time with the two-mode approximation and about 500 s with the full analysis (using an IBM 3090 in vectorized mode).

Deterministic and Probabilistic Design Formulations

The objective of the optimizations is to limit the largest accelerations at specific nodes and within prescribed frequency windows. The design variables can include design parameters of the damping devices and the truss itself, as well as the locations of the damping devices on the structure. In actual structures some or all design variables as well as other parameters of the model are uncertain. They are considered random variables in the probabilistic approach. Only the nominal (mean) values of the design variables and model parameters are used in the deterministic approach. The same resource limits are used in both formulations. Our goal is to evaluate experimentally the gain in reliability (or equivalently, reduction in probability of failure) when using the probabilistic formulation vs the deterministic optimization for the truss design problem.

We consider the following scenario: the truss has been designed with one damper for each mode (modes 1 and 3 only) to limit dynamic response accelerations. A large number of trusses and dampers have been manufactured and samples have been tested. The tests have revealed a significant mistuning of the dampers that will result in poor overall performance of the damped structure. We assume that the dampers cannot be modified to improve their tuning. However, tuning masses can be easily added to the nodes of the truss to modify its natural frequencies and improve tuning. These tuning masses have a fixed magnitude (16.6 g), and to limit the added weight, a maximum of 10 masses can be used. Also, the locations of the two dampers on the structure can be modified. The problem consists of optimally redesigning the system by adding tuning masses and moving the dampers to ensure satisfactory performance.

We assume that the properties of the truss are deterministic, because the same truss is used for all realizations of the complete system. By adjusting the stiffnesses and loss factors of the nine springs (see Fig. 3), as well as the loss factor of the structural members (assumed to be the same for all members) we can match the measured natural frequencies and damping ratios of the structure without dampers or tuning masses. With this assumption, the parametric uncertainties in the system are limited to the properties of the tuned absorbers and the different realizations of the system are created by attaching different copies of the dampers to the same truss.

The response is measured at the nodes and in the directions that correspond to the largest acceleration amplitudes in the first and third modes in the original undamped truss. The excitation is assumed to have a flat spectrum and a unit amplitude. This allows us to use transfer functions from excitation force to response accelerations as a substitute for the accelerations themselves. The transfer functions $H^{(1)}$ and $H^{(3)}$ corresponding to the two measurement points are defined as

$$H^{(1)}(i\omega) = \frac{\ddot{u}^{(1)}(i\omega)}{f(i\omega)} \tag{3}$$

$$H^{(3)}(i\omega) = \frac{\ddot{u}^{(3)}(i\omega)}{f(i\omega)} \tag{4}$$

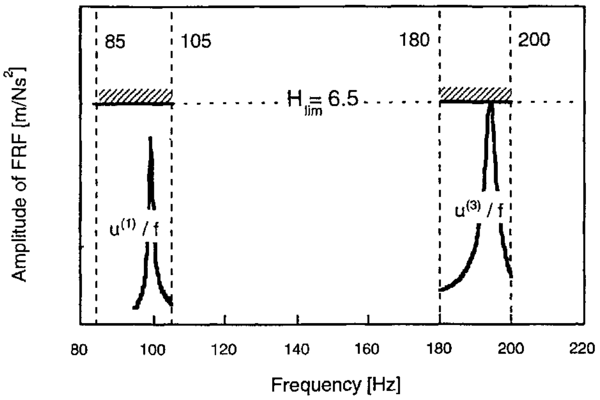

Fig. 5 Frequency windows and amplitude limits.

where $u^{(1)}$ and $u^{(3)}$ are displacements, f is the excitation force, ω is the frequency, $i = \sqrt{(-1)}$, and a dot denotes differentiation with respect to time.

The upper limits on $H^{(1)}$ and $H^{(3)}$ are set to the same level H_{lim} (i.e., $H_{\text{lim}}^{(1)} = H_{\text{lim}}^{(3)} = H_{\text{lim}}$) in two frequency windows, covering the two modes of interest (modes 1 and 3). This is illustrated in Fig. 5.

The optimization problem then consists of finding optimal locations of a maximum of 10 added masses and optimal locations and directions for one damper of each type to limit the magnitude of the transfer function at the specified response measurement points.

The deterministic formulation seeks to maximize the safety margin α associated with the limit on the acceleration. It can be formulated as

$$\underset{\substack{\text{damp. loc., damp. dir.,}\\ \text{mass loc.}}}{\text{Maximize}} \qquad \alpha = H_{\text{lim}} - \max\left[H_{\text{peak}}^{(1)}, H_{\text{peak}}^{(3)}\right] \tag{5}$$

such that number of masses ≤ 10, where $H_{\text{peak}}^{(1)}$ and $H_{\text{peak}}^{(3)}$ stand for the peak value of $H^{(1)}$ in the first frequency window, which covers the neighborhood of the first mode, and the peak value of $H^{(3)}$ in the second frequency window, which covers the neighborhood of the third mode. They are evaluated for nominal (mean) damper properties. A negative value of the safety margin α corresponds to a design that violates at least one of the constraints on response accelerations. The use of the max function leads to nonsmooth objective function that creates numerical difficulties for gradient-based optimizers but not for genetic algorithms.

The corresponding probabilistic formulation minimizes the probability P_f that the transfer function peak can exceed a threshold H_{lim}:

$$\underset{\substack{\text{damp. loc., damp. dir.,}\\ \text{mass loc.}}}{\text{Minimize}} \qquad P_f = P\left[H_{\text{peak}}^{(1)} \geq H_{\text{lim}} \text{ or } H_{\text{peak}}^{(3)} \geq H_{\text{lim}}\right] \tag{6}$$

such that number of masses ≤ 10.

Genetic Optimization

The deterministic and the probabilistic optimizations use the same 14 design variables: the locations of the 2 dampers, the orientation of these 2 dampers on the node, and the locations of a maximum of 10 masses.

We use the standard mounting holes of the nodes to attach the dampers so that only nine discrete directions are feasible. The locations of the masses and dampers are restricted to the nodes of the truss so that all 14 design variables are discrete. For this reason we used genetic algorithms for the optimizations. The same algorithm is used for the deterministic and probabilistic cases; only the objective function differs. All deterministic analyses and Monte Carlo simulations were performed using the two-mode models and approximate mode shapes. The approximate mode shapes are obtained from the mode shapes of the original truss (without dampers or tuning masses), using a first-order correction for the effect of the tuning masses.

The genetic algorithm uses the three classical genetic operators (selection, crossover, and mutation) and an elitist strategy where the best individual of a population is always cloned into the next generation. The selection uses the ranking technique where the probability of selection of an individual is proportional to one plus the population size minus its rank in the population. Details on the genetic optimization algorithm can be found in Ref. 12.

Contrast Maximization

Our goal is to evaluate the difference in reliability between the deterministic and the probabilistic approach. Measuring probabilities of failure in the laboratory is time consuming, and measuring very small probabilities or very small differences in probabilities of failure requires a prohibitively large number of experiments. For this reason, we had to identify a design problem that leads to alternative designs with a significant difference in probabilities of failure. To find such a design problem we carried on a process known as antioptimization[7–11] (because it often seeks conditions that make one model look bad) or contrast maximization, because it maximizes the contrast between the two design approaches.

Antioptimization requires a number of problem parameters that can be varied to achieve the increased contrast. For our problem we selected the mean values of the natural frequencies of the two types of dampers (the amount of mistuning), the failure limit H_{lim} (the stringency of the requirements), and the relative magnitudes of the scatter in the parameters of the two types of dampers. The antioptimization process was also performed with the aid of genetic algorithms (see Ref. 12 for details).

The contrast maximization procedure identified the following problem that gives the largest difference between the probabilities of failure of the probabilistic design and that of the deterministic design: type-1 dampers should have an average natural frequency of 110 Hz (overtuned) with a small coefficient of variation of about 1.5%, type-3 should have a mean natural frequency of about 182 Hz (undertuned) with a coefficient of variation of about 3.5%, and the failure limit H_{lim} should be equal to 6.5 m/s^{2}N. The optimum deterministic and probabilistic designs will represent different compromises between improving the behavior of mode 3 and degrading the behavior of mode 1 (since adding masses can only reduce natural frequencies).

Results

Damper Parameters

We manufactured 29 dampers of each type. The parameters of these dampers were measured once after fabrication. The statistical distributions of the measured parameters were approximately normal but did not exhibit the desired mean values and standard deviations (as determined from the contrast maximization procedure). For the natural frequency, which is the most important parameter affecting the performance of the dampers, we wanted to obtain the desired distribution. To achieve this we sampled these distributions with a uniform step size in probability. We then evaluated approximate adjustments of the tip screws of the individual dampers that would realize these desired distributions. The dampers were then adjusted and remeasured. Therefore, the resulting samples of dampers are not random samples; rather, they are discretized representations of the desired distribution of the natural frequency. The preceding procedure is along the lines of stratified sampling.[18] Obviously, the distributions of the other damper parameters were also altered by the adjustment of the tip screws.

Because the dampers use viscoelastic foam, their characteristics depend strongly on temperature. The effect of temperature changes on the identified parameters was measured to be about 9%/°C on the loss factor, −0.9%/°C on the natural frequency, and 0.7%/°C on the identified tip masses. To protect ourselves from this effect, we use a temperature stabilization system that maintains the temperature of the laboratory at 24.4°C (76°F) on average with a rapid oscillation of ±0.8°C (±1.5°F). The period of that oscillation is about 15 min. All measurements are repeated three times and averaged to reduce the effect of the small temperature oscillation and other measurement errors.

The resulting samples of parameters were used to evaluate the means, standard deviations, coefficients of variation, and correlation coefficients between parameters for both types of dampers. Tables 1

Table 1 Type-1 dampers, statistics (sample of 29) of tip mass m, natural frequency f_n, and loss factor η

	Parameter		
	m	f_n	η
Mean	7.075 g	109.97 Hz	0.12604
COV, %	1.11	1.59	5.37
Correlation coefficients			
m	1.000	——	——
f_n	0.693	1.000	——
η	0.689	0.375	1.000

Table 2 Type-3 dampers, statistics (sample of 29) of tip mass m, natural frequency f_n, and loss factor η

	Parameter		
	m	f_n	η
Mean	7.340 g	180.16 Hz	0.15811
COV, %	1.29	3.09	6.32
Correlation coefficients			
m	1.000	——	——
f_n	0.697	1.000	——
η	0.511	0.016	1.000

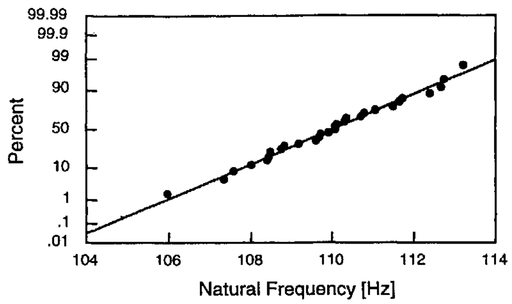

Fig. 6 Distribution of type-1 dampers natural frequencies. Straight line is root-mean-square fit corresponding to normal distribution.

and 2 list these values for types 1 and 3, respectively. Figure 6 shows a normal probability plot of the measured distribution of the natural frequencies of the 29 type-1 dampers. The scale used on the probability axis is such that a perfectly normally distributed sample would lie on a straight line. The respective plots for the remaining two random parameters of type-1 dampers and for all three parameters of type-3 dampers look similar. The figure shows that the normalcy assumption used in the statistical analysis is justified.

Validation and Calibration of Analytical Models

We performed two series of tests on a few dampers of each type, chosen among the 29 available to cover the whole range of the parameter distributions. The parameters of each damper were measured three times and averaged to reduce experimental errors and temperature effects. The resulting sets of parameters were used to predict analytically the peak of the frequency response curve of the original truss (no tuning masses) with a damper at the location and in the direction corresponding to the largest amplitude in its target mode. The peak amplitudes were then measured. Again, the measurements were repeated three times and averaged. The coefficient of correlation between analytical and experimental results was equal to 98.4% for type-1 and 99.8% for type-3. This indicates that the model of the truss is precise. However there was a systematic mismatch between experimental measurements and numerical predictions, which was detected when straight lines were fitted to the experimental and analytical results. The results of both the full analysis and the two-mode model were corrected using a linear transformation to account for that systematic mismatch. The equations used for the correction of the two-mode model are as follows.

Type-1 damper:

$$H_{\text{corr}} = 0.94 H_{\text{anal}} - 0.71 \tag{7}$$

Type-3 damper:

$$H_{\text{corr}} = 1.28 H_{\text{anal}} - 0.46 \tag{8}$$

where H_{anal} is the analytically obtained peak of the frequency response and H_{corr} the corresponding corrected value.

Tuning Masses

We used 10 standard steel screws and nuts as tuning masses. Their average mass is equal to 16.61 g with a sample COV, corresponding to 10 samples, of about 0.4%. This very small scatter was neglected so that the tuning masses were considered deterministic. Even when all 10 tuning masses are added to the truss, the added mass represents less than 3.8% of the mass of the original truss.

Optimization Results

During the optimizations, all analyses were performed using the two-mode approximation. The final designs were then reanalyzed using the full analysis. A deterministic optimum was obtained with mean values for the damper parameters shown in Tables 1 and 2. The deterministic design uses a total of seven masses. Six masses are attached to node 7 and one to node 10. Type-1 and type-3 dampers are attached to nodes 12 and 11, respectively. Since we minimize the largest of these amplitudes and we do not penalize for the number of tuning masses used in the design, the amplitudes of the two modes tend to equalize in the optimum design.

The nominal amplitudes evaluated with the two-mode approximation are 4.408 m/Ns^2 for mode 1 and 4.438 m/Ns^2 for mode 3. This corresponds to a safety margin of 2.062 m/Ns^2 from the limit of 6.5 m/Ns^2. Reevaluated with the full analysis, the nominal amplitudes are 4.395 m/Ns^2 for mode 1 and 4.172 m/Ns^2 for mode 3. The probabilities of failure evaluated using Monte Carlo simulation with 1000 samples and the two-mode approximation are 0% for mode 1 and 17.5% for mode 3. The system probability of failure is 17.5%. Reevaluated with the full analysis the probabilities of failure are 0% for mode 1 and 15.3% for mode 3. The system probability of failure is 15.3%. Note the large difference in probabilities of failure between the two failure modes. This is because although the deterministic optimization uses a uniform safety margin for all failure modes the scatter of mode 3 is considerably larger than that of mode 1 (see Fig. 7).

Using the data of Tables 1 and 2 for the statistics of the parameters, we performed the probabilistic optimization. The final system probability of failure was equal to 0.4% (0.1% for mode 1 and 0.3% for mode 3) as evaluated with the two-mode approximation. The same design, reanalyzed with the full analysis, gives a probability of failure of 0.6% (0.1% for mode 1 and 0.5% for mode 3). Again, the difference is small enough to justify the use of the two-mode approximation in the optimization. The probabilistic optimum design uses all 10 tuning masses. One of these masses is attached to node 7 and nine to node 10. The damper locations are the same as in the deterministic design. The nominal peak amplitudes of the probabilistic design (evaluated with the two-mode approximation) are 5.000 m/Ns^2 for mode 1 and 2.290 m/Ns^2 for mode 3. This corresponds to a safety margin of 1.500 m/Ns^2 from the limit of 6.5 m/Ns^2. Notice that the probabilistic design has a substantially reduced safety margin compared with the deterministic design.

Figure 7 compares the deterministic and probabilistic designs. Specifically, the figure shows the histograms of the peak amplitudes of the two failure modes (from Monte Carlo simulation with the two-mode approximation) for each design. The dashed vertical line in each histogram represents the failure limit ($H_{\text{lim}} = 6.5$ m/Ns^2). For the deterministic design, all failures occur in the third mode, due to the large scatter in the response of that mode. The first mode, on the other hand, has been given too wide a safety margin; the tail of the distribution is just touching the failure limit.

The probabilistic design represents another compromise for the same design problem: the safety margin has been tailored to the magnitude of the scatter in each mode. Compared with the deterministic design, three more masses have been used. This has considerably reduced the nominal peak amplitude of the third mode while slightly degrading the response of the first mode. Notice also that the scatter in mode 3 has been reduced.

Table 3 Deterministic and probabilistic designs, comparison of experimental (sample of 29) and analytical results (Monte Carlo, sample of 1000, two-mode approximation)

	Deterministic		Probabilistic	
	Analytical	Experimental	Analytical	Experimental
Mode 1, %	0.0	0.0	0.1	3.5 (1 of 29)
Mode 3, %	17.5	17.2 (5 of 29)	0.3	0.0
Total, %	17.5	17.2 (5 of 29)	0.4	3.5 (1 of 29)
[$\pm 1\sigma$ interval]	[16.3 ... 18.7]		[0.2 ... 0.6]	

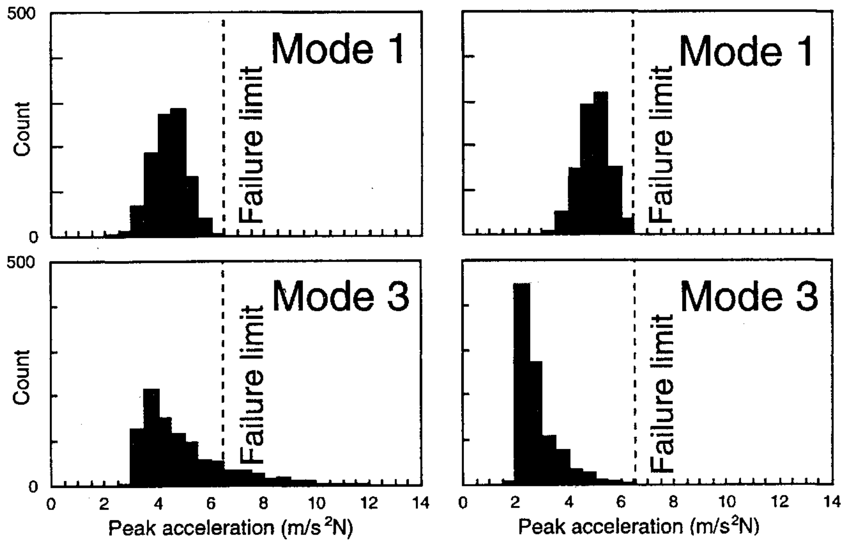

Fig. 7 Deterministic (left) and probabilistic (right) designs: distributions of peak amplitudes (Monte Carlo, sample of 1000, two-mode approximation).

Experimental Results

We prepared 29 sets of two absorbers by randomly selecting one damper of each type (all dampers were used and none was used twice). These 29 sets were used to create 29 realizations of each design. Each realization was tested three times in the laboratory and the measured peak amplitudes were averaged through the three measurements (this averaging is intended to reduce the effect of measurement errors and temperature changes). The probabilities of failure were evaluated from these 29 values for each design by counting the number of designs that violate the requirement on the peak amplitudes. With a sample of 29 measurements, the resolution of the probability measurement is about 3.45%. Since the difference in reliability between the two designs is 17.1%, this resolution is sufficient to measure the difference experimentally.

The results of the experiment are presented in Table 3. The experimental probabilities of failure of the deterministic and probabilistic designs are compared with predicted values from Monte Carlo simulations using 1000 points and the two-mode approximation. We have also included in this table intervals of $\pm 1\sigma$ on the total probability of failure. The standard deviation of the obtained probability of failure was calculated using Eq. (2). We observe that the experimental probabilities are within resolution error from the analytical predictions.

Figures 8 and 9 show the cumulative probability curves for the two failure modes of the deterministic and probabilistic designs, respectively. Note that experimental results and analytical predictions are close.

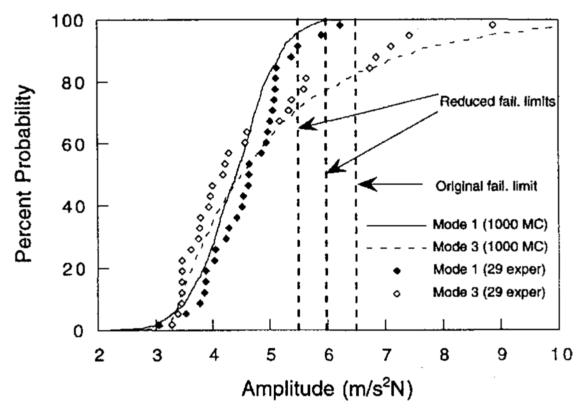

Fig. 8 Deterministic design: cumulative distributions.

Sensitivity to Errors

It is observed from Fig. 9 that the probabilistic design is very sensitive to the failure limit, which means that it is also sensitive to modeling errors that result in underestimation of the transfer function. For example, if we lower the failure limit from 6.5 to 6.0 $\mathrm{m/Ns^2}$, the probability of failure, according to the experimental results, will become 20.7% (6 failures out of 29 realizations)—an increase of 17.2%. A similar behavior is observed from the analytical results, the only difference being that we need to lower the limit to about 5.5 $\mathrm{m/Ns^2}$ to see that the design is sensitive. Specifically the failure probability increases from 0.4 to 19.7% when the failure limit reduces from 6.5 to 5.5 $\mathrm{m/Ns^2}$. This sensitivity can be explained by the sharp form of the probability density function of mode 1 and its high value at the failure limit (see Fig. 7). Note that probability density is the derivative of distribution, and so if the density is high at the failure limit, the probability will increase considerably if that limit is reduced.

To reduce sensitivity to modeling error, we tried to model this error by multiplying the analytically predicted transfer functions by a normally distributed random variable with a mean value of 1.0 and a COV of 15%. These statistics represent an estimate of the modeling error based on the experimental results. We then performed a probabilistic optimization including the modeling uncertainties in the analysis. The new optimum design was just slightly different from the previous probabilistic optimum. One tuning mass moved from node 10 to node 7, the new design had two masses on node 7 and eight on node 10, and the damper locations were the same. The probability of failure of the new design was 6.3% at $H_{\lim} = 6.5\ \mathrm{m/s^2N}$ and 30.9% at $H_{\lim} = 5.5\ \mathrm{m/s^2N}$. The corresponding values of the original design (reanalyzed including modeling uncertainties) were 6.6 and 31.6%, respectively. Thus, no significant improvement of

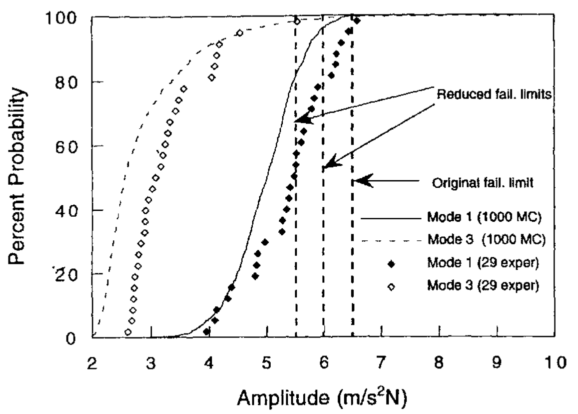

Fig. 9 Probabilistic design: cumulative distributions.

the sensitivity was achieved by including the modeling uncertainties in the model.

We then tried to include the sensitivity of the probability of failure explicitly in the objective function of the probabilistic optimization by modifying the objective of Eq. (6) as follows:

$$\underset{\text{damp. loc., damp. dir., mass loc.}}{\text{Minimize}} \quad wP_f + (1-w)[P_f(5.5) - P_f(6.5)] \tag{9}$$

where w is a weighting parameter, representing a compromise between probability of failure and sensitivity to errors.

We performed a probabilistic optimization using the compromise objective function and a value of $w = 0.333$. The compromise optimal design had seven tuning masses at node 7 and three at node 10. The locations of the dampers were the same as in the previous designs. At $H_{\text{lim}} = 6.5$ m/s^{2}N the compromise design had a significantly lower probability of failure (6.6%) than its deterministic counterpart (17.5%). However, at $H_{\text{lim}} = 5.5$ m/s^{2}N the probability of failure of the compromise design (19.1%) is only slightly better than that of the original design (19.7%), and so the compromise design is less sensitive than the original design, but most of the gain in sensitivity occurred at the expense of the probability of failure at $H_{\text{lim}} = 6.5$ m/s^{2}N. Therefore, we cannot really say that the compromise design is better than the original design.

We believe that our inability to reduce the sensitivity of the probabilistic design without a significant loss of performance is due to two factors. First, the problem is rather simple with only two failure modes and a single dominant random variable (tuning frequency). Second, the design problem was optimized to maximize the difference between the probabilities of failure of the probabilistic and deterministic designs.

Concluding Remarks

We have presented an analytical and experimental comparison of probabilistic and deterministic design approaches for a damped structure. The main sources of uncertainties have been identified and their statistical properties evaluated from measurements. Two alternative designs corresponding to the same design problem have been obtained from deterministic and probabilistic optimizations and their reliabilities have been compared on the basis of analysis and experiments. A combination of genetic algorithms, an efficient analytical approximation analysis, and Monte Carlo simulations has been used for the optimization. We have shown that, in some cases, very large gains in reliability can be achieved by minimizing failure probabilities instead of maximizing safety factors. The predicted gains in reliability were validated in the laboratory by performing repeated measurements on several realizations of deterministic and probabilistic optimum designs.

However, we also found that the success of probabilistic optimization depends on the quality of the models available and the statistical information about the uncertainties in the system. If the quality of the models and the statistical information is not sufficient, the actual reliability of a probabilistic design is not guaranteed to exceed that of a deterministic design.

Acknowledgments

Partial support for this work was provided by NASA Langley Research Center under Grants NAG-1-224 and NAG-1-1458. The authors also wish to thank W. K. Belvin and W. J. Stroud of NASA Langley Research Center for their assistance in providing some of the experimental equipment.

References

[1]Frangopol, D. M., and Moses, F., "Reliability Based Structural Optimization," *Advances in Design Optimization*, edited by H. Adeli, 1st Ed., Chapman and Hall, New York, 1994, Chap. 13.

[2]Yang, J.-S., Nikolaidis, E., and Haftka, R. T., "Design of Aircraft Wings Subjected to Gust Loads: A System Reliability Approach," *Computers and Structures*, Vol. 36, No. 6, 1990, pp. 1057–1066.

[3]Ponslet, E., Haftka, R. T., Hallauer, W. L., and Cudney, H. H., "Desensitizing Structural-Control Design," *Journal of Guidance, Control, and Dynamics*, Vol. 17, No. 1, 1994, pp. 175–180.

[4]Sepulveda, A. E., "Structural Synthesis with Reliability Constraints Using Approximation Concepts," *Proceedings of the AIAA/ASME/ASCE/AHS/ASC 35th Structures, Structural Dynamics, and Materials Conference* (Hilton Head, SC), AIAA, Washington, DC, 1994, pp. 833–841.

[5]Ben-Haim, Y., and Elishakoff, I., *Convex Models of Uncertainty in Applied Mechanics*, Elsevier, Amsterdam, 1990.

[6]Elishakoff, I., and Hasofer, A. M., "Effect of Human Error on Reliability of Structures," *Proceedings of the AIAA/ASME/ASCE/AMS/ASC 33rd Structures, Structural Dynamics, and Materials Conference* (Dallas, TX), AIAA, Washington, DC, 1992, pp. 3233–3237.

[7]Haftka, R. T., and Kao, P. J., "The Use of Optimization for Sharpening Differences Between Models," Presented at the Winter Annual Meeting (Dallas, TX), American Society of Mechanical Engineers, New York, 1990.

[8]Gangadharan, S. N., Nikolaidis, E., Lee, K., and Haftka, R. T., "The Use of Antioptimization to Compare Alternative Structural Models," *Proceedings of the AIAA/ASME/ASCE/AHS/ASC 34th Structures, Structural Dynamics, and Materials Conference* (La Jolla, CA), AIAA, Washington, DC, 1993, pp. 534–542.

[9]van Wamelen, A., Johnson, E. R., and Haftka, R. T., "Optimal Design of Laminated Specimens to Evaluate Competing Composite Failure Criteria," *Proceedings of the 8th Technical Conference*, American Society for Composites, Cleveland, OH, 1993, pp. 1045–1055.

[10]Elishakoff, I., "On the Uncertainty Triangle," *The Shock and Vibration Digest*, Vol. 22, No. 10, 1990, p. 1.

[11]Elishakoff, I., "Convex Versus Probabilistic Modeling of Uncertainty in Structural Dynamics," *Structural Dynamics: Recent Advances*, edited by M. Petyt, H. F. Wolfe, and C. Mei, Elsevier, London, 1991, pp. 3–21.

[12]Ponslet, E., "Analytical and Experimental Comparison of Probabilistic and Deterministic Optimization," Ph.D. Dissertation, Dept. of Aerospace Engineering, Virginia Polytechnic Inst. and State Univ., Blacksburg, VA, 1995.

[13]Anon., *MATLAB User's Guide*, The MathWorks, Inc., Natick, MA, 1992.

[14]Hasselman, T. K., and Ross, J. D., "Propagation of Modeling Uncertainty Through Structural Dynamic Models," *Proceedings of the AIAA/ASME/ASCE/AHS/ASC 35th Structures, Structural Dynamics, and Materials Conference* (Hilton Head, SC), AIAA, Washington, DC, 1994, pp. 72–83; see also AIAA Paper 94-1316, April 1994.

[15]Maglaras, G., and Nikolaidis, E., "Integrated Analysis and Design in Stochastic Optimization," *Structural Optimization*, Vol. 2, No. 3, 1990, pp. 163–172.

[16]Fox, E. P., "Methods of Integrating Probabilistic Design Within an Organization's Design System Using Box-Behnken Matrices," *Proceedings of the AIAA/ASME/ASCE/AHS/ASC 34th Structures, Structural Dynamics, and Materials Conference* (La Jolla, CA), AIAA, Washington, DC, 1993, pp. 714–723.

[17]Melchers, R. E., *Structural Reliability, Analysis and Prediction*, Ellis Horwood, Chichester, England, UK, 1987, pp. 93, 94.

[18]McKay, M. D., Beckman, R. J., and Conover, W. J., "A Comparison of Three Methods for Selecting Values of Input Variables in the Analysis of Output from a Computer Code," *Technometrics*, Vol. 21, No. 2, 1979, pp. 239–245.